Acta Neuropathol (1990) 80:581–589

Acta Neuropathologica

Laminar distribution of neuron degeneration in posterior cingulate cortex in Alzheimer's disease*

B. A. Vogt[1, 2], G. W. Van Hoesen[3], and L. J. Vogt[1, 2]

[1] Department of Anatomy, Boston University School of Medicine 80 East Concord Street, Boston, MA 02118, USA
[2] Veterans Administration Hospital, 200 Springs Road, Bedford, MA 01730, USA
[3] Departments of Anatomy and Neurology, University of Iowa, College of Medicine Iowa City, IA 52242, USA

Received January 10, 1990/Revised April 17, 1990/Accepted May 4, 1990

Summary. The laminar distribution of neuron losses in posterior cingulate cortex were evaluated in 25 clinically and neuropathologically diagnosed cases of dementia of the Alzheimer type (DAT). The layer of maximal neuron loss in area 23a for each DAT case was determined by comparison with mean neuron densities for each layer of 17 neurologically intact control cases. The DAT cases were separated into five classes: class 1, 12% of all DAT cases, no or less than 40% neuron loss in any layer; class 2, 24%, maximal neuron losses in layers II or III; class 3, 28%, losses mainly in layer IV; class 4, 12%, losses mainly in layers V or VI; class 5, 24%, severe losses in all layers. An analysis of large and small neurons showed that in class 2 there was an equal loss of both in layer IIIa–b, in class 3 mostly small neurons were lost in layer IV, in class 4 mostly large neurons were lost in layers III, IV and V, while in class 5 there was no selectivity. The age of disease onset and length of the disease were the same for all classes, although classes 4 and 5 tended to have an earlier onset. No measures of thioflavin S-stained neuritic plaque (NP) or neurofibrillary tangle (NFT) density discriminated among these classes. In 64% of all DAT cases there was a progressive shift in NFT from ventral area 30 where most were in layer II to areas 23a–b where there was a balance between those in superficial and deep layers to dorsal area 23c where most were in layers V and VI. There were four cases with massive numbers of NFT in area 23a (1802 ± 477 versus 261 ± 44 for all other cases). Since one of these cases was in each of classes 1, 2, 3 and 5, it is unlikely that this form of amyloid deposition is related to laminar specificities in neuron degeneration. Finally, neuron and NFT densities in the hippocampal formation were the same for each class. In conclusion, differential laminar changes in neuron density provide a basis for neuropathological subtyping of DAT which is more sensitive than measures of thioflavin S-stained NP and NFT densities either in neocortex or the hippocampus.

Key words: Cerebral cortex – Neuron degeneration – Neuritic plaques – Neurofibrillary tangles

Neuropathological alterations in neocortical neurons have been documented in dementia of the Alzheimer type (DAT) including a rate of neuron loss greater than that of normal aging and formation of neurofibrillary tangles (NFT). These studies have concluded that either large or small neurons are involved in DAT pathogenesis. Degeneration of large neurons, i.e., presumably pyramidal projection cells, has been demonstrated in temporal, frontal and cingulate neocortices [33, 45] and this loss is highly correlated with severity of the dementia [34]. Also, neocortical layers III and V contain the largest cortical neurons and it is in these layers of temporal cortex that a 60% loss of neurons occurs [25], although these investigators did not analyze other layers. Most NFT occur in neurons in layers III and V [22, 35]. Finally, large neurons in layers II and III of entorhinal cortex which project into the hippocampal formation degenerate in DAT [18, 19].

In addition to the above reports of large neuron losses, there is evidence for loss of small neurons in DAT, i.e., presumably those with primarily intracortical projection fields. Braak and Braak [6] employed lipofuscin pigment granules to define pyramidal and nonpyramidal neuron types and found that in area 11, i.e., in the gyrus rectus and adjacent orbitofrontal cortex, there was a 30% loss of nonpyramidal neurons and no change in the number of pyramidal neurons. Immunochemical and receptor binding studies have also implicated alterations in small populations of interneurons including somatostatinergic [3, 12, 15, 32, 36, 38, 39] and neuropeptide Y-containing [9] neurons.

* Supported by NIH-NINDS grants NS18745, NS14944 and PONS19632

Offprint requests to: B. A. Vogt, Department of Physiology and Pharmacology, Bowman Gray School of Medicine, Wake Forest University, 300 South Hawthorne Road, Winston-Salem, NC 27103, USA

In hippocampal cortex there is a strong and negative correlation between pyramidal cell loss and NFT and neuritic plaque (NP) formation [2, 25]. A similar relationship holds in neocortex [25, 33] and one study [25] reported that in elderly patients neuron loss and the density of NFT and NP in neocortex can be lower than in younger cases; thus, NFT and NP formation in neocortex is not correlated with the duration of the disease. In a study of a variety of neocortical areas in six DAT cases it was found that neuron losses ranged from none to 80% [8]. These observations suggest that neurons in the hippocampus are systematically destroyed in all cases of DAT, while those in neocortex are destroyed in either a graded, progressive sequence or according to unique subtypes. The analysis of Brun and Englund [8] was based on a graded scale from a rating of 0 with no neuron loss nor gliosis to a grade of 4 with extensive neuron loss and gliosis. However, based on the findings of Mann et al. [25] that earlier onset cases have greater neuron loss and the fact that Brun and Englund's [8] most severe case had an onset at age 45, while the least severe case had an onset at age 86.5, it is possible that neocortical changes reflect different classes and fundamentally different pathogenic processes rather than gradation of a unitary process.

A number of clinical subtypes of DAT have been proposed and one of the most crucial markers is the age of disease onset. Since there is a bimodal distribution of the frequency of age of onset [10, 28] and individuals who express the disease earlier have a shorter relative survival time [43], DAT cases can be divided into early onset, i.e., at or before age 65, or late onset for those expressing the disease after age 65. Early onset cases usually have the most severe intellectual decline and tend to have greater language dysfunction or mutism than do late onset cases [10, 13, 28, 43]. Early onset cases also have a greater proportion of myoclonus and extrapyramidal signs [10, 13, 28] and neurochemical disturbances, which are greater than in late onset cases. These latter disturbances include major reductions in the acetylcholine synthetic enzyme choline acetyltransferase [4] and metabolites of dopamine and serotonin including homovanillic acid and 5-hydroxyindoleacetic acid, respectively [14, 21].

Although it has recently been shown that increased numbers of NFT and NP occur in visual cortex in DAT patients [7, 37] some with deficits in visuospatial skills [17], it is unclear what the relationship is between clinical subtypes of DAT and alterations in cortical neuron density. Mountjoy et al. [33] and Mann et al. [25] showed that earlier onset was associated with greater neuron losses, however, their age cutoff was 80. Duffy et al. [13] did not quantify neuron density, but in four of 27 cases with myoclonus and mutism the mean age of onset was about 57 and there was a "paucity of neurons" which is also attested to in their figures. Braak and Braak [6] showed a loss of 30% of nonpyramidal neurons in area 11 in six early onset cases with no changes in pyramidal neurons.

If two or more neuropathological classes of DAT can be distinguished in neocortex, cingulate cortex is one of the regions in which they will most likely be expressed. For example, comparison of mild and severe DAT cases [8] showed that of nine areas surveyed posterior cingulate cortex had the widest variation in neuron loss, from 2% to 79% of control values, respectively. The strategy of the present study is to determine the layers of posterior cingulate cortex in which the greatest relative loss of neurons occurs in comparison to age-matched control cases. It was found that neurons are preferentially lost in different layers of some cases, that these losses are not progressive from mild to severe cases, that there are no simple relationships among neuron, NFT and NP densities and that large and small neurons are lost in different proportions depending upon the layer in which neuron losses were most prevalent. In a subsequent article the fidelity of this classification scheme will be evaluated in terms of an analysis of neurotransmitter receptor alterations in these classes of DAT.

Materials and methods

The posterior cingulate cortices of 42 patients were analyzed. Twenty-five had a clinical history and cortical neuropathology consistent with DAT. Seventeen, age-matched cases were used as controls. These latter cases had no clinical history of dementia or other neurological disorders. None had NFT and only two (cases 19 and 20) had a small number of NP in posterior cingulate cortex. Histories for each of these cases are presented in Table 1.

As noted in Table 1, cingulate cortices of 12 DAT and 8 control cases were formalin fixed and 13 DAT and 9 control cases were prepared without fixation. This latter series was employed for in vitro receptor binding studies (Vogt et al., submitted for publication). Blocks from these latter cases were frozen to $-70°C$ and stored at this temperature. They were cut in a cryostat at a 48-μm thickness, i.e., three times the 16-μm thickness which was used for receptor binding studies, mounted on chrome-alum subbed slides and stained with either thionin or thioflavin S [41]. Formalin-fixed cases were placed in a solution of 4% formalin, 10% sucrose and 10% glycerol until the blocks were saturated and sank. The blocks were cut serially at a 50-μm thickness on a freezing microtome. One in every ten sections was stained with thionin and another one in ten series was stained for thioflavin S.

Cell density was evaluated in the following manner. The perikarya of thionin-stained neurons with nucleoli were drawn from 160-μm-wide strips of cingulate cortex using a drawing tube attached to a microscope. The identification of each cytoarchitectonic area was based on studies of monkey and human posterior cingulate cortex [5, 49, 52, 55]. A final magnification of $\times 330$ was used for the fixed series and $\times 650$ for the unfixed series; the latter magnification was used because it allowed for more consistent detection of nucleoli and cell boundaries in unfixed cells. Glial cells were not drawn. They were usually less than 8 μm in diameter, had pale-staining nuclei and a limited cytoplasm. Neurons were subdivided into large and small categories in which large neurons were defined as those with a width greater than 12 μm and included all of the large neurons which are typically used to define the cytoarchitectural extent of layers IIIc and Va. Small neurons had perikaryal profiles ≤ 12 μm. Two strips of cortex were drawn for each area and the boundaries of each layer confirmed at lower magnification ($\times 100 - \times 200$). The final drawings were between 2.5 and 6.5 feet in length. The total number of perikarya in each layer were counted for each strip and a mean value calculated for each case. The mean number of neurons $\pm$ SEM in each layer was then determined separately for control cases in the fixed and unfixed series. Classification of each DAT case was based on which layer had the largest percentage neuron loss when compared to one of the matched control groups. The two series of DAT cases were then standardized so that statistical analysis could be performed. The multiple comparison protected t test [11] was used to compare control groups with classes of

Table 1. History of cases

Fixed cases	Age at death	Age at onset	Sex	PMI (h)	Brain weight (g)	Cause of death
Alzheimer's disease						
Case 1	65	55	F	5	947	Bronchopneumonia
2	82	72	M	6	1094	Bronchopneumonia
3	88	73	F	2	1084	Bronchopneumonia
4	79	74	F	11	1074	Congestive heart failure
5	83	71	M	24	1168	NA
6	90	85	F	4	1067	Renal failure
7	75	72	F	24	1013	Thromboembolism
8	69	59	F	8	1239	NA
9	74	62	F	4	971	Bronchopneumonia
10	58	50	F	3	1083	Dehydration
11	64	58	M	5	1109	Cardiopulmonary arrest
12	67	50	M	12	1350	Cardiopulmonary arrest
	75 ± 3	65 ± 3		9 ± 2	1100 ± 32	
Control						
Case 13	61	–	M	11	1179	Carcinoma, lung
14	80	–	F	3	1078	Carcinoma liver
15	75	–	F	5	1173	Carcinomatosis
16	70	–	F	NA	1203	Carcinoma, breast
17	61	–	F	24	1355	Aortic aneurysm
18	72	–	M	7	1428	Carcinoma, esophagus
19	80	–	M	8	1207	Cardiac arrest
20	79	–	F	10	1072	Congestive heart failure
	72 ± 3			10 ± 2	1212 ± 44	
Unfixed cases						
Alzheimer's disease						
Case 21	84	78	M	17	1170	Cardiopulmonary arrest
22	70	62	M	3	1250	Bronchopneumonia
23	65	60	M	4	1300	Volvulus of small intestine
24	78	72	M	3	NA	Bronchopneumonia
25	79	71	M	5	1100	Bronchopneumonia
26	60	54	F	16	1090	Bronchopneumonia
27	72	63	M	2	890	Bronchopneumonia
28	70	62	M	5	1340	Bronchopneumonia
29	62	52	M	3	950	Bronchopneumonia
30	71	67	M	4	1345	Bronchopneumonia
31	67	60	M	3	1150	Bronchopneumonia
32	78	65	M	4	1050	Bronchopneumonia
33	67	59	M	9	1180	Bronchopneumonia
	71 ± 2	64 ± 2		6 ± 1	1151 ± 42	
Control						
Case 34	82	–	M	15	1340	Pulmonary embolism
35	66	–	F	17	1120	Aortic aneurysm
36	62	–	M	16	1380	Carcinoma, lung
37	73	–	M	6	1440	Carcinoma, lung
38	73	–	M	16	1240	Pulmonary embolism
39	56	–	M	13	1480	Myocardial infarct
40	65	–	F	8	1240	Myocardial infarct
41	77	–	M	13	1150	Carcinoma, prostate
42	61	–	M	10	1420	Myocardial infarct
	68 ± 3			13 ± 1	1312 ± 43	

PMI, postmortem interval; NA, not available

DAT cases each having unequal numbers of subjects. The computer program for this test was produced by Dynamic Microsystems, Inc. (Silver Spring, MD). Correlation coefficients were also used to assess relationships between neuron density and clinical factors and other measures of neuropathology. A $P < 0.01$ was accepted as significant for differences among means. The two control series were compared and it was found that there were always more neurons per layer in the fixed series according to the following factors for area 23a: layer II, 2.25; IIIa–b, 1.67; IIIc, 1.6; IV, 3.53; Va, 1.5; Vb, 1.9; VI, 1.6. Thus to compensate for differences in neuron density due to differences in tissue preparation, the above factors were used to standardize the two series of DAT cases. The basic classification of cases, however, was not dependent on this correction.

Densities of NP and NFT were assessed in cingulate cortex in the following way. A microscope with epifluorescence was used which had a 380–425-nm excitation filter and a 450-nm absorption filter. The X and Y axes of the stage were coupled to potentiometers which provided coordinates for each NP and NFT to an IBM AT

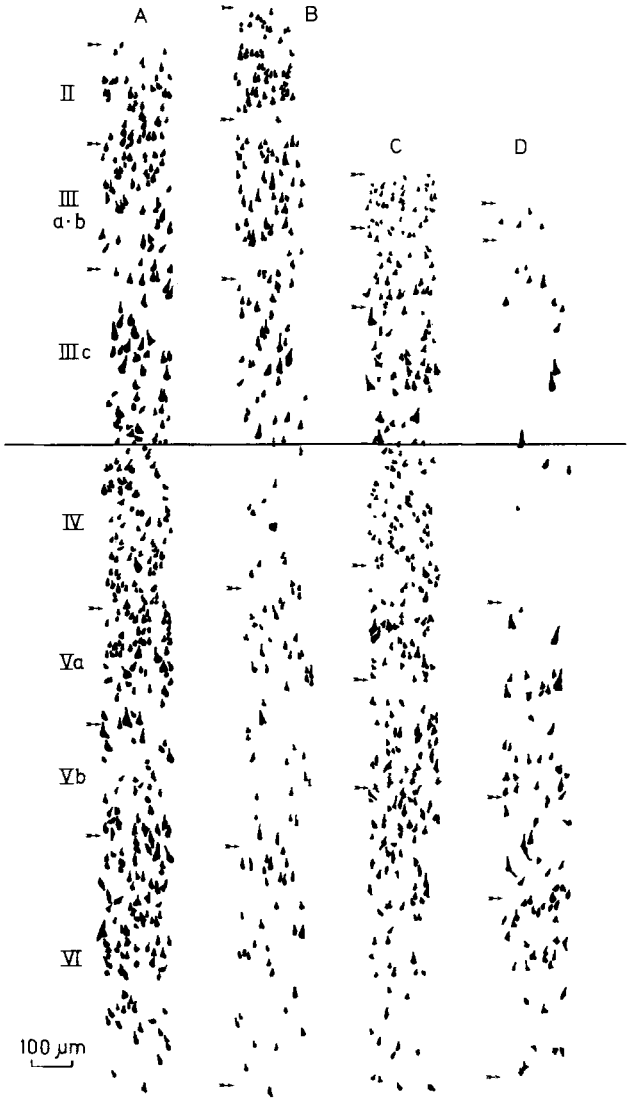

Fig. 1. Drawings of neuronal perikarya in strips of area 23a showing examples of neuron losses in different layers. The drawings were aligned at the layer IIIc/IV border as indicated with the solid line. *A* Control case 15. *B* Case 6 is an example of class 3 damage. *C* Case 3 is an example of class 2 damage. *D* In case 11 neuron losses are severe in all layers as is generally true for class 5, although layers V and VI are still present

computer. Once the distribution of NP and the section outline were recorded, a Hewlett-Packard plotter was used to print this information onto opaque paper. The distribution of NFT was then plotted and printed on translucent paper so that each representation of NP and NFT could be directly matched for a particular case. Adjacent thionin-stained sections were drawn at the same magnification and were used for estimating the locations of cortical layers. The location of NFT in subdivisions of layers III and V were beyond the resolution of this system. The densities of NP and NFT were either determined for an entire area or by layer for the area in a single transverse section or per mm^2 for superficial and deep layers. In the latter instance, a digitized electronic pad (Micro-plan II, Donsanto Corp., Natick, MA, USA) was used to estimate the area of layers I – IV and layers V and VI and then the number of NP and NFT calculated per mm^2. For DAT cases in which the hippocampal formation was available for thioflavin S staining (n = 21), NFT and neurons with nucleoli were plotted on the system described above. A 3-mm strip through that part of the CA1, prosubiculum/subiculum was chosen which had the highest density of NFT. The total number of NFT and neurons were reported for this 3-mm width of cortex. All means are reported ±SEM.

Results

It was apparent from a survey of drawings through area 23a like those in Fig. 1 that, although there was a generalized loss of neurons, in many cases particular layers were damaged severely. Fig. 1 B is a drawing from a case in which layers IV – VI were more severely involved than layers II – IIIc. In Fig. 1 C neuron density was close to normal in layers IV – VI, however, neurons in layers II and IIIa – b were particularly shrunken and reduced in number. In some cases, as in Fig. 1 D, neuronal losses were so severe that layers II – IV were not present, though remnants of layers V and VI were retained.

A classification scheme was developed to account for the wide range of neuronal losses in posterior cingulate cortex. As described in the Materials and methods, the number of neurons in each layer of a DAT case was compared to the mean number of neurons in a group of age-matched control cases prepared histologically in the same manner. If neuron density for a DAT case was equal to or above that of the control cases or had losses of less than 40%, it was assigned to class 1. As shown in Table 2, 3 of the 25 cases were in this class. These cases were essentially the same as control cases except for layer VI which had more neurons than in control cases. In six of the DAT cases percentage neuron losses were greatest in layers II or III. Neuron degeneration in these cases was limited to layer IIIa – b as shown in Table 2. Cases were placed in class 3 which had most neuron losses in layer IV. These cases had an additional reduction in neuron density in layer VI. Class 4 was composed of DAT cases with most neuron degeneration in layers V or VI. Finally, six of the DAT cases had such severe neuron losses that the architecture of many layers was lost. It was still possible to make approximations of laminar boundaries in these cases because there were always a few remaining large layer IIIc and layer Va pyramidal neurons. As shown in Table 2, significant losses of neurons occurred in all layers of class 5 cases.

The drawings of neuronal perikarya were analyzed in terms of small and large neurons, i.e., those with a width up to 12 µm versus those with a width >12 µm, respectively. This analysis was limited to layers III – V because these are the main layers on which the classification scheme was based and because there are almost no large neurons in layers II and VI. Table 3 presents the mean values for all control and DAT cases. According to this analysis the differences in neuron density between control and class 1 cases could be accounted for by the presence of more small neurons in class 1. This was not due to shrinkage because all 3 class 1 cases were frozen. In class 2 there was an approximately equal loss of large and small neurons in layer IIIa – b, while in class 3 the loss of small neurons accounted for the bulk of neuronal losses in layer IV. In class 4 large neurons were lost in layers IIIc, IV and Va. Finally, large and small neurons were lost throughout most layers of class 5 cases.

Table 2. Neuron density in area 23a

	II	IIIa–b	IIIc	IV	Va	Vb	VI
Control							
$n = 17$	62 ± 4	76 ± 6	55 ± 4	67 ± 5	59 ± 3	35 ± 2	113 ± 6
Class 1: no loss							
$n = 3$ (12% of DAT cases)	62 ± 12	76 ± 12	66 ± 10	96 ± 23	62 ± 4	63 ± 17	162 ± 16*
Class 2: layers II or III							
$n = 6$ (24% of DAT cases)	44 ± 6	30 ± 3*	37 ± 4	53 ± 6	44 ± 3	33 ± 5	94 ± 11
Class 3: layer IV							
$n = 7$ (28% of DAT cases)	47 ± 4	55 ± 8	48 ± 6	24 ± 3*	41 ± 5	32 ± 5	82 ± 12*
Class 4: layers V or VI							
$n = 3$ (12% of DAT cases)	55 ± 8	60 ± 6	49 ± 11	42 ± 14	26 ± 7*	21 ± 5	62 ± 4*
Class 5: severe							
$n = 6$ (24% of DAT cases)	8 ± 2*	18 ± 4*	20 ± 4*	7 ± 3*	11 ± 3*	9 ± 2*	40 ± 5*

* $P < 0.01$ compared to control values
DAT, Dementia of Alzheimer type

Table 3. Large and small neurons in area 23a

	IIIa–b Large/small	IIIc Large/small	IV Large/small	Va Large/small	Vb Large/small
Control	12 ± 1/66 ± 6	15 ± 1/39 ± 3	5 ± 1/62 ± 5	10 ± 1/48 ± 3	8 ± 1/27 ± 2
Class 1	10 ± 3/75 ± 14	11 ± 1/57 ± 11	2 ± 1/97 ± 22*	5 ± 2/65 ± 2	7 ± 2/58 ± 15*
Class 2	*5 ± 1/26 ± 3*	11 ± 1/26 ± 3	4 ± 1/46 ± 8	8 ± 2/35 ± 3	5 ± 1/28 ± 5
Class 3	10 ± 2/47 ± 7	15 ± 2/31 ± 5	3 ± 1/19 ± 4*	6 ± 1/34 ± 5	5 ± 1/27 ± 5
Class 4	6 ± 1/48 ± 6	*7 ± 2/44 ± 10	*3 ± 1/36 ± 12	*2 ± 1/22 ± 7	3 ± 1/17 ± 4
Class 5	*4 ± 1/15 ± 3*	*8 ± 1/12 ± 3*	*1 ± 0.3/6 ± 3*	*3 ± 0.3/8 ± 3*	*1 ± 0.3/7 ± 2

* $P < 0.01$ compared to control values

Table 4. Summary of case data by class

	Length of disease	Age at onset	NFT Area 23a	NP		CA1/subiculum	
				Area 23a	Layer I	Neuron density	NFT
Class 1	6.3 ± 0.9	67 ± 6	733 ± 185	136 ± 19	51 ± 36	641 ± 93	112 ± 86
Class 2	9.2 ± 1.4	67 ± 4	767 ± 473	240 ± 49	46 ± 35	194 ± 81	252 ± 41
Class 3	7.6 ± 1.1	68 ± 4	388 ± 258	157 ± 41	61 ± 24	321 ± 77	183 ± 37
Class 4	9.3 ± 1.9	61 ± 2	286 ± 157	58 ± 4	21 ± 12	291 ± 135	315 ± 76
Class 5	9.2 ± 2	58 ± 3	389 ± 158	186 ± 69	31 ± 18	348 ± 63	296 ± 51

NFT, Neurofibrillary tangles; NP = neuritic plaques

In terms of clinical course, the age at disease onset and length of the disease were not correlated and did not differ among the five classes. Table 4 presents the means ± SEM for these variables by class. Although cases in classes 4 and 5 tended to have an earlier age at disease onset, these differences were not significant. In addition, in control cases neuron density was correlated with age at death only in layer IV for which there was a correlation coefficient of −0.64. This correlation with age at death was not present in DAT cases.

The density of thioflavin S-stained NP did not differentiate among the classes whether measured in terms of number per mm^2 for superficial or deep layers, total NP in area 23a, number of NP in each layer of area 23a or number of NP in layer I of all areas in the cingulate gyrus. Only one variable correlated with NP density and that was the density of NFT ($r = 0.76$, $P = 0.0001$).

Neurofibrillary tangles were distributed in two qualitatively different patterns in posterior cingulate cortex, each of which is illustrated in Fig. 2. In the typical pattern, i.e., 16 of 25 cases, most NFT in area 30 were in layer II with a few also in layer V. In areas 23a and 23b there was an approximately equal density in layers II and III versus layers V and VI, while in area 23c most NFT were in layers V and VI. Thus, there was a progressive shift from superficial to deep layers in ventral to dorsal parts of cingulate cortex. In the second pattern most NFT were in deep layer III and layer IV, while few were in layers V and VI. This distribution was basically the same for area 30 and subdivisions of area 23. Only in area 29 were more

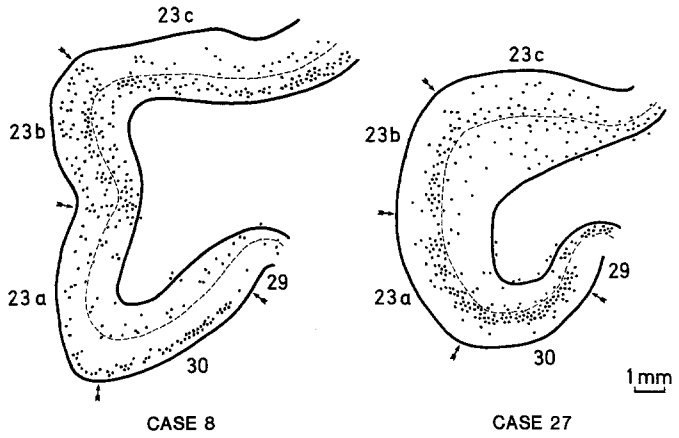

Fig. 2. Two distribution patterns of NFT in posterior cingulate cortex; each dot is equal to approximately three NFT. *Case 8* is an example of the shifting pattern in which most NFT are in superficial layer II of ventral area 30, equal numbers are in superficial and deep layers of areas 23a and 23b and dorsal area 23c has most NFT in deep layers V and VI. *Case 27* is an example of a pattern which is more constant across the cingulate gyrus in which most NFT are in layers IIIc and IV. The dashed lines indicate the border between layers IV and V

NFT in the deep than superficial layers, while in area 23c there was a more homgeneous distribution. This latter pattern was observed in four cases. Finally, two cases had NFT in layers III and V with slightly higher densities in deeper layers, while three cases had almost no NFT. The three cases with no NFT were in class 3, while all class 5 cases had the typical pattern.

In four cases there were more than 1000 NFT in a coronal section of area 23a (1802 ± 477 versus 261 ± 44 for all other cases). One of these cases was in each of classes 1, 2, 3 and 5. Thus, the deposition of NFT in these cases was probably not related to laminar specificity in neuron death. In addition, there were no differences in age of disease onset nor length of the disease between these two groups of cases.

The hippocampal formation was available for thioflavin S staining in 21 of the DAT cases. The peak density of NFT in the CA1 and/or prosubicular/subicular sectors for each class is presented in Table 4, as are neuron densities recorded from adjacent, thionin-stained sections. There were no diffrences among these classes in the densities of NFT nor neurons in the hippocampal formation.

Table 5 presents neuron densities for area 30 by class. As a general rule class 1 had the least neuron degeneration and class 5 the most severe degeneration, while cases in classes 2 and 3 had less severe damage than that in area 23a. Mean differences with $P < 0.05$ showed that area 30 had systematic neuron losses in layer IIIa–b for all but class 1 cases. Analysis of area 23a data with a similar P standard did not uncover a similar effect. Finally, area 30 often had more NFT in layer II than in any other cingulate area. If NFT formation and neuron degeneration are closely related events, it might be expected that cases with a high number of NFT in layer II also would have high levels of neuron degeneration regardless of the area 23a classification scheme. Neuron density in layer II was calculated for the ten cases with high densities of NFT in layer II, i.e. those cases with the shifting pattern depicted in Fig. 2, and for nine other cases excluding those in class 5. There were the same number of neurons in each group with 41 ± 3 versus 38 ± 5 neurons, respectively.

Discussion

Cases of DAT can be classified into five groups according to the layer(s) in which neurons degenerate in area 23a of posterior cingulate cortex. No measures of thioflavin S-stained NP or NFT distinguish among these classes and similar measures of pathology in the hippocampal formation do not distinguish among them. There are two reasons why it is unlikely that these classes represent a simple gradation from no neuron losses in class 1 to severe losses in class 5. First, the laminar pattern of degeneration is not compatible with a simple progression. For example, layer IIIa–b neuron degeneration in class 2 could follow that in class 1 and degeneration in class 5 could follow that in class 2. However, classes 3 and 4 have a normal number of neurons in layer IIIa–b. Second, the age at disease onset and length of the disease are the same for all classes and there is no correlation between age at death and neuron density. In fact, the most severe cases in class 5 tend to have an earlier onset than the less severely damaged cases in classes 1 and 2.

It is possible that dysfunction and/or patent neuron losses in cingulate cortex contribute to the clinical course of DAT, particularly disruption of mnemonic processes. It is well established in experimental animals that cingulate cortex contributes to the acquisition and performance of active avoidance and spatial memory tasks [16, 23, 24, 27, 44] and may contribute to processes that require attention [53]. Recently Valenstein et al. [47] described a case of "retrosplenial amnesia" in which a small infarct in cingulate cortex around the splenium of the corpus callosum resulted in both retrograde and anterograde amnesia. Certainly class 5 cases of the present series can be viewed as having virtually total removal of posterior cingulate cortex. Although cases in classes 2, 3 and 4 express a more restricted pattern of neuron loss, they may have sufficient losses to disconnect key components of circuits involved in memory function such as those which link anterior thalamic and temporal neocortical areas.

Most morphometric studies of neocortical neuron loss in DAT have emphasized losses of large pyramidal neurons particularly those in layers III and V [25, 45]. The densities of these neurons are highly correlated with the severity of the dementia [34] and neurons in layers III and V are most likely to form NFT (e.g., [35]). However, DAT is not a disease of large neurons alone. As noted in the introduction a number of studies have implicated interneurons in the progress of DAT. Also, some quantitative studies have only sampled large neurons in layers III and V and formation of NFT may be misleading as it may not be the only factor which leads to neuron death. Findings of the present study point to significant

Table 5. Neuron density in area 30

	II	IIIa–b	IIIc	IV	Va	Vb	VI
Control	56 ± 3	78 ± 5	72 ± 6	60 ± 4	44 ± 4	29 ± 2	89 ± 5
Class 1	48 ± 1	78 ± 7	73 ± 13	44 ± 4	45 ± 4	23 ± 1	76 ± 2
Class 2	40 ± 4	58 ± 5*	60 ± 8	45 ± 8	34 ± 8	24 ± 3	67 ± 6*
Class 3	41 ± 6	58 ± 9*	52 ± 9*	41 ± 11*	32 ± 3	16 ± 1	70 ± 7*
Class 4	26 ± 4*	42 ± 12**	41 ± 4*	29 ± 7*	30 ± 1	15 ± 3	62 ± 4*
Class 5	20 ± 8**	30 ± 12**	22 ± 8**	17 ± 7**	13 ± 6**	16 ± 3	52 ± 8**

* $P < 0.05$; ** $P < 0.01$ compared to control values

involvement of small neurons, many of which are likely small pyramidal neurons as well as interneurons. Class 3 is defined by greatest proportionate loss of neurons in layer IV which contains almost no large pyramidal neurons. Furthermore, losses in layer IIIa–b of class 2 cases involved large and small neurons equally. Finally, the severe losses in all layers of class 5 cases cannot be accounted for solely on the basis of large neuron losses.

There have been reports of cases that are similar to class 1 of the present study in which no neuron loss could be detected in neocortex [8, 25]. In fact, there were more neurons in layers V and VI than in control cases in the present study. This was not due to cortical shrinkage, as all three cases were frozen and not processed further. Since there were only three cases in class 1, it is premature to conclude that a class of DAT actually has more neurons. However, it is possible that removal of cortical afferents in this class reduces the extent of deep layer neuropil thus indirectly changing neuron density. A similar phenomena has been noted experimentally by Saunders and Duda (in preparation) who have shown that ablation of the fornix in monkey alters neuron density in the mammillary bodies secondary to neuropil changes. Finally, it is possible that individuals with class 1 DAT will be amenable to drug therapies should a clinical correlate or diagnostic assay become available for identifying such individuals. To the extent that the clinical course of DAT is dependent on neocortical neuropathological changes, therapies for cases in classes 4 and 5 are much less likely to be successful.

Densities of NFT did not distinguish among the five classes of DAT cases in the present study. Four cases had particularly high densities of NFT and were evenly distributed among the classes supporting the notion that amyloid deposition does not necessarily occur in direct conjunction with neuron degeneration. These latter cases raise the possibility that two types of NFT form in cingulate cortex. In most cases NFT either form transiently and disappear or never form in the first place. In a limited number of cases, insoluble NFT form which can survive neuron degeneration as is the case for NFT in entorhinal and hippocampal cortices.

Since the pathogenesis of some classes of DAT is layer specific, it is reasonable to expect that features of the clinical presentation might reflect dysfunction in particular layers. Categories of functions can be delineated by the projections of neurons in specific layers. In broadest terms, neurons in layer III project mainly but not exclusively to cortical sites and are likely involved in sensorimotor integration and memory, while layer V neurons project predominantly to motor structures and so are likely involved in triggering appropriate motor responses. More specifically, layer III neurons of posterior cingulate cortex have intracingulate connections, i.e., those within posterior cingulate cortex such as between areas 30 and 23, those to anterior cingulate cortex and those to contralateral cingulate cortex [1, 51]. Layer III and some layer V neurons also project to parahippocampal and inferior parietal neocortices [1, 29]. Projections of layer V neurons into the somatic and autonomic motor systems include those to motor and supplementary motor cortices [30], the pontine and caudate nuclei [40, 48, 54] and the periaqueductal gray [26, 31]. Additionally, although layer VI neurons project to limbic thalamus including the anterior and laterodorsal nuclei [20, 41], these neurons are not selectively lost in DAT but are involved along with those in other layers in classes 3, 4 and 5. In conclusion, it is possible that cases in classes 1 and 2 will express deficits more closely associated with sensorimotor integration and mnemonic processes, while class 4 would have additional deficits in targeting and sequencing motor outputs.

Although evidence in the present study suggests that the five classes of cingulate cortical neuropathology are at least partially independent, a number of questions regarding the progression and clinical nature of DAT remain unanswered. First, do class 5 cases pass rapidly through some combination of classes 1, 2, 3, and 4 in the course of the disease accumulating a series of laminar-specific changes which result in a homogeneous loss of neurons or is there a homogeneous loss of neurons throughout all layers during the development of class 5 pathology which is never laminar specific? Second, neuron death is a cumulative phenomenon which can be measured in end-stage cases. Since NFT and NP do not distinguish among these classes, are there other factors contributing to layer-specific neuron death, possibly not involving amyloid deposits? Finally, what is the contribution of specific laminar pathologies to the clinical course of dementia in each of the five classes?

Acknowledgements. We thank Drs. Ladislav Volicer, Thomas Kemper and Bradley Hyman for their comments and suggestions on aspects of this research. We also thank the following individuals for their assistance in providing samples of cingulate cortex from Alzheimer and/or control cases: Loren Spence at the University of Iowa School of Medicine, Iowa City, IA; Drs. Devay Lathi and Chompol Mahaesian at the Veterans Administration Hospital, Bedford, MA; Dr. Edward Bird at the Brain Tissue Resource Center,

McLean Hospital, Belmont, MA; Dr. Judith Marquis at Boston University School of Medicine, Department of Pharmacology and Dr. J. Ulrich at the Institut für Pathologie der Universität Basel, Basel, Switzerland.

References

1. Baleydier C, Mauguiere F (1980) The duality of the cingulate gyrus in monkey. Neuroanatomical study and functional hypothesis. Brain 103:525–554
2. Ball MJ (1977) Neuronal loss, neurofibrillary tangles and granulovacuolar degeneration in the hippocampus with ageing and dementia. Acta Neuropathol (Berl) 37:111–118
3. Beal MF, Mazurek MF, Tran VT, Chattha G, Bird ED, Martin JB (1985) Reduced numbers of somatostatin receptors in the cerebral cortex in Alzheimer's disease. Science 229:289–291
4. Bird TD, Stranahan S, Sumi SM, Raskin M (1983) Alzheimer's disease: choline acetyltransferase activity in brain tissue from clinical and pathological subgroups. Ann Neurol 14:284–293
5. Braak H (1979) Pigment architecture of the human telencephalic cortex IV. Regio retrosplenialis. Cell Tissue Res 204:431–440
6. Braak H, Braak E (1986) Ratio of pyramidal cells versus non-pyramidal cells in the human frontal isocortex and changes in ratio with ageing and Alzheimer's disease. Prog Brain Res 40:185–212
7. Braak H, Braak E, Kalus P (1989) Alzheimer's disease: areal and laminar pathology in the occipital isocortex. Acta Neuropathol 77:494–506
8. Brun A, Englund E (1981) Regional pattern of degeneration in Alzheimer's disease: neuronal loss and histopathological grading. Histopathology 5:549–564
9. Chan-Palay V, Lang W, Allen YS, Haesler U, Polak JM (1985) II. Cortical neurons immunoreactive with antisera against neuropeptide Y are altered in Alzheimer's-type dementia. J Comp Neurol 238:390–400
10. Chui HC, Teng EL, Henderson VW, Moy AC (1985) Clinical subtypes of dementia of the Alzheimer type. Neurology 35:1544–1550
11. Couch JV (1982) Fundamentals of statistics for the behavioral sciences, St Martin's Press, New York, pp 266–270
12. Davies P, Katzman R, Terry RD (1980) Reduced somatostatin-like immunoreactivity in cerebral cortex from cases of Alzheimer disease and Alzheimer senile dementia. Nature 288:279–280
13. Duffy P, Mayeux R, Kupsky W (1988) Familial Alzheimer's disease with myoclonus and 'spongy change'. Arch Neurol 45:1097–1100
14. Ebinger G, Bruyland M, Martin JJ, Herregodts P, Cras P, Michotte Y, Gomme L (1987) Distribution of biogenic amines and their catabolites in brains from patients with Alzheimer's disease. J Neurol Sci 77:267–283
15. Ferrier IN, Crass AJ, Johnson JA, Roberts GW, Crow TJ, Corsellis JAN, Lee YC, O'Shaughnessy D, Adrian TE, McGreger GP, Baracese-Hamilton AJ, Bloom SR (1983) Neuropeptides in Alzheimer type dementia. J Neurol Sci 62:159–170
16. Gabriel M, Foster K, Orona E, Saltwick SE, Stanton M (1980) Neuronal activity of cingulate cortex, anteroventral thalamus, and hippocampal formation in discriminative conditioning: encoding and extraction of the significance of conditional stimuli. Prog Psychobiol Physiol Psychol 9:125–231
17. Hof PR, Bouras C, Constantinidis J, Morrison JH (1989) Balint's syndrome in Alzheimer's disease: specific disruption of the occipito-parietal visual pathway. Brain Res 493:368–375
18. Hyman BT, Van Hoesen GW, Kromer LJ, Damasio AR (1986) Perforant pathway changes and the memory impairment of Alzheimer's disease. Ann Neurol 20:472–481
19. Hyman BT, Kromer LJ, Van Hoesen GW (1988) A direct demonstration of the perforant pathway terminal zone in Alzheimer's disease using the monoclonal antibody Alz-50. Brain Res 450:392–397
20. Kaitz SS, Robertson RT (1981) Thalamic connections with limbic cortex II. Corticothalamic projections. J Comp Neurol 195:527–545
21. Kaye JA, May C, Attack JR, Daly E, Sweeney DL, Beal MF, Kaufman S, Milstein S, Friedland RP, Rapoport SI (1988) Cerebrospinal fluid neurochemistry in the myoclonic subtype of Alzheimer's disease. Ann Neurol 24:647–650
22. Lewis DA, Campbell MJ, Terry RD, Morrison JH (1987) Laminar and regional distributions of neurofibrillary tangles and neuritic plaques in Alzheimer's disease: a quantitative study of visual and auditory cortices. J Neurosci 7:1799–1808
23. Lubar JF (1964) Effect of medial cortical lesions on the avoidance behavior of the cat. J Comp Physiol Psychol 58:38–46
24. Lubar JF, Perachio AA (1965) One-way and two-way learning and transfer of an active avoidance response in normal and cingulectomized cats. J Comp Physiol Psychol 60:46–52
25. Mann DMA, Yates PO; Marcyniuk B (1985) Some morphometric observations on the cerebral cortex and hippocampus in presenile Alzheimer's disease, senile dementia of the Alzheimer type and Down's syndrome in middle age. J Neurol Sci 69:139–159
26. Mantyh PW (1982) Forebrain projections to the periaqueductal gray in the monkey, with observations in cat and rat. J Comp Neurol 206:146–158
27. Matsunami K, Kawashima T, Satake H (1989) Mode of [^{14}C]2-deoxy-D-glucose uptake into retrosplenial cortex and other memory-related structures of the monkey during a delayed response. Brain Res Bull 22:829–838
28. Mayeux R, Stern Y, Spanton S (1985) Heterogeneity in dementia of the Alzheimer type: evidence of subtypes. Neurology 35:453–461
29. Mesulam M-M, Van Hoesen GW, Pandya DN, Geschwind N (1977) Limbic and sensory connections of the inferior parietal lobule (area PG) in the rhesus monkey: a study with a new method for horseradish peroxidase histochemistry. Brain Res 136:393–414
30. Morecraft RJ, Van Hoesen GW (1988) Somatotopical organization of cingulate projections to the primary and supplementary motor cortices in the old-world monkey. Neurosci Abstr 14:820
31. Morrell JI, Greenberger LM, Pfaff DW (1981) Hypothalamic, other diencephalic, and telencephalic neurons that project to the dorsal midbrain. J Comp Neurol 201:589–620
32. Morrison JH, Rogers J, Scherr S, Benoit R, Bloom FE (1985) Somatostatin immunoreactivity in neuritic plaques of Alzheimer's patients. Nature 314:90–92
33. Mountjoy CQ, Roth M, Evans NJR, Evans HM (1983) Cortical neuronal counts in normal elderly controls and demented patients. Neurobiol Aging 4:1–11
34. Neary D, Snowdon JS, Mann DMA, Bowen DM, Sims NR, Northern B, Yates PO; Davison AN (1986) Alzheimer's disease: a correlative study. J Neurol Neurosurg Psychiatry 49:229–237
35. Pearson RCA, Esiri MM, Hiorns RW, Wilcock GK, Powell TPS (1985) Anatomical correlates of the distribution of the pathological changes in the neocortex in Alzheimer disease. Proc Natl Acad Sci USA 82:4531–4534
36. Roberts GW, Crow TJ, Polak JM (1985) Location of neuronal tangles in somatostatin neurones in Alzheimer's disease. Nature 314:92–94
37. Rogers J, Morrison JH (1985) Quantitative morphology and regional and laminar distributions of senile plaques in Alzheimer's disease. J Neurosci 5:2801–2808
38. Rossor MN, Emson PC, Mountjoy CQ, Roth M, Iversen LL (1980) Reduced amounts of immunoreactive somatostatin in the temporal cortex in senile dementia of Alzheimer type. Neurosci Lett 20:373–377
39. Rossor MN, Iversen LL, Reynolds GP, Mountjoy CQ, Roth M (1984) Neurochemical characteristics of early and late onset types of Alzheimer's disease. Brit. Med. J 288:961–964

40. Royce GJ (1982) Laminar origin of cortical neurons which project upon the caudate nucleus: a horseradish peroxidase investigation in the cat. J Comp Neurol 205:8–29
41. Royce GJ (1983) Cells of origin of corticothalamic projection upon the centromedian and parafascicular nuclei in the cat. Brain Res 258:11–21
42. Schwartz PH, Kurucz J, Kurucz A (1964) Recent observations on senile cerebral changes and their pathogenesis. J Am Geriat Soc 12:908–922
43. Seltzer B, Sherwin I (1983) A comparison of clinical features in early and late onset primary degenerative dementia one entity or two? Arch Neurol 40:143–146
44. Sutherland RJ, Whishaw IQ, Kolb B (1988) Contributions of cingulate cortex to two forms of spatial learning and memory. J Neurosci 8:1863–1872
45. Terry RD, Peck A, DeTeresa R, Schechter R, Horoupian S (1981) Some morphometric aspects of the brain in senile dementia of the Alzheimer type. Ann Neurol 10:184–192
46. Terry RD, Hansen LA, DeTeresa R, Davies P, Tobias H, Katzman R (1987) Senile dementia of the Alzheimer type without neocortical neurofibrillary tangles. J Neuropathol Exp Neurol 46:262–268
47. Valenstein E, Bowers D, Verfaellie M, Heilman KM, Day A, Watson RT (1987) Retrosplenial amnesia. Brain 110:1631–1646
48. Vilensky JA, Van Hoesen GW (1981) Corticopontine projections from the cingulate cortex in the rhesus monkey. Brain Res 205:391–395
49. Vogt BA (1976) Retrosplenial cortex in the rhesus monkey: a cytoarchitectonic and Golgi study. J Comp Neurol 169:63–98
50. Vogt BA (1985) Cingulate cortex. In: Peters A, Jones EG (eds) Cerebral Cortex, vol 4. Plenum Publishing, New York, pp 89–149
51. Vogt BA, Pandya DN (1987) Cingulate cortex of the rhesus monkey II. Cortical afferents. J Comp Neurol 262:271–289
52. Vogt BA, Pandya DN, Rosene DL (1987) Cingulate cortex of the rhesus monkey I. Cytoarchitecture and thalamic afferents. J Comp Neurol 262:256–270
53. Watson RT, Heilman KM, Cauthen JC, King FA (1973) Neglect after cingulectomy. Neurology 23:1003–1007
54. Yeterian EH, Van Hoesen GW (1978) Cortico-striate projections in the rhesus monkey: the organization of certain cortico-caudate connections. Brain Res 139:43–63
55. Zilles K, Armstrong E, Schlaug G, Schleicher A (1986) Quantitative cytoarchitectonics of the posterior cingulate cortex in primates. J Comp Neurol 253:514–524